

# Finding Gravitational Lenses With X-rays

J. A. Muñoz, C. S. Kochanek & E. E. Falco

Harvard-Smithsonian Center for Astrophysics, 60 Garden St., Cambridge, MA 02138

email: jmunoz, ckochanek, efalco@cfa.harvard.edu

## ABSTRACT

There are  $\sim 1$ ,  $0.1$  and  $0.01$  gravitationally lensed X-ray sources per square degree with soft X-ray fluxes exceeding  $10^{-15}$ ,  $10^{-14}$  and  $10^{-13}$  ergs  $s^{-1}$   $cm^{-2}$  respectively. These sources will be detected serendipitously with the Chandra X-ray Observatory at a rate of 1–3 lenses per year of high resolution imaging. The low detection rate is due to the small area over which the HRC and ACIS cameras have the  $< 1''.5$  FWHM resolution necessary to find gravitational lenses produced by galaxies. Deep images of rich clusters at intermediate redshifts should yield one wide separation ( $\Delta\theta \gtrsim 5''.0$ ) multiply-imaged background X-ray source for every  $\sim 10$ ,  $30$  and  $300$  clusters imaged to the same flux limits.

*Subject headings:* cosmology: theory – gravitational lensing – cosmology: observations – quasars: general – X-rays: galaxies

## 1. INTRODUCTION

Gravitational lenses are an increasingly powerful tool for studies of cosmology (Falco, Kochanek & Muñoz 1998, Cooray 1999, Helbig 1999), the Hubble constant (Impey et al. 1998, Barkana et al. 1999, Bernstein & Fischer 1999, Fassnacht et al. 1999), galactic structure (Keeton, Kochanek & Falco 1998) and galactic evolution (Kochanek et al. 1999). Their utility is growing at a fast pace because the number of known lenses is increasing rapidly, having reached  $\sim 50$  systems at present (see <http://cfa-www.harvard.edu/castles>). Despite the larger samples, we have discovered only a small fraction of the total number of lenses detectable with modern instruments.

Confusion is a fundamental problem for existing gravitational lens surveys. Even at high Galactic latitudes, most point sources found near quasars are stars rather than gravitationally lensed images (see Kochanek 1993a). Confusion in radio lens surveys is caused by the range of source structures – flat-spectrum radio lens surveys contain far more compact doubles than

two-image lenses (see Helbig et al. 1999), and steep-spectrum surveys must cope with the enormous variety of extended radio-emission morphologies (e.g., Griffith et al. 1991). These problems vanish for high-resolution X-ray imaging observations, where confusing Galactic sources are rare (as at radio wavelengths) and source structure is simple (as for quasars). However, the image separations in lenses are small – of the nearly 50 known lenses, 90% are larger than  $0''.5$ , the median separation is  $1''.5$ , and only 10% are larger than  $2''.5$  (Keeton et al. 1998) – thus, high angular resolution (of order  $1''$ ) is required. The resolution problem can be avoided by looking for lensed images produced by rich clusters, where the image separation is much larger (e.g., Luppino et al. 1999).

The High Resolution Camera (HRC) and the AXAF CCD Imaging Spectrometer (ACIS) on the Chandra X-ray Observatory will allow the first direct searches for gravitational lenses at X-ray wavelengths. Both HRC and ACIS combine a relatively wide field of view with high spatial resolution near the center of the field (50% enclosed energy radius  $r_{50} \simeq 0''.5$ ). Unfortunately, the resolution worsens with the distance from the field center  $D$ , with  $r_{50} \simeq 0''.5 + 6''.0(D/10')^2$  (see Kenter et al. 1997), and only the central portion of the detector will be useful for recognizing the typical lensed source. In §2 we estimate the probability of lensing X-ray emitting AGN as a function of flux, including rough estimates of the observational selection effects for the HRC and ACIS detectors. In §3 we estimate the probability of finding lensed X-ray AGN in fields centered on massive clusters at intermediate redshift, where the larger image separations make the worsening resolution at large off-axis angles relatively unimportant. We summarize our conclusions in §4.

## 2. SERENDIPITOUS LENSES

The method for calculating the expected number of lenses is well developed; we follow the calculations used for the radio lens surveys by King & Browne (1996), Kochanek (1996), Falco, Kochanek & Muñoz (1998), Cooray (1999) and Helbig et al. (1999). We assume that the lens galaxies are described by singular isothermal spheres (SIS) with parameter normalizations derived from the best fits to the multiply-imaged radio sources and quasars in Kochanek (1996) and Falco et al. (1998). The SIS mass distribution is generally consistent with the available lens data (see, e.g., Kochanek 1995), as well as local stellar dynamical measurements (Rix et al. 1997) and X-ray observations (e.g., Fabbiano 1989) of early-type galaxies. We ignore spiral galaxy lenses, as they are a small fraction of all lenses (10–20%) and produce  $\simeq 50\%$  smaller image separations (see Kochanek 1996). We describe the early-type lens galaxies by a constant comoving Schechter (1976) luminosity function

$$\frac{dn}{dL} = \frac{n_*}{L_*} \left( \frac{L}{L_*} \right)^\alpha \exp(-L/L_*) \quad (1)$$

and a Faber-Jackson (1976) relation to convert from luminosity to velocity dispersion,

$$\frac{L}{L_*} = \left( \frac{\sigma}{\sigma_*} \right)^\gamma. \quad (2)$$

The parameters  $n_* = 0.0061h^3 \text{ Mpc}^{-3}$ ,  $\alpha = -1.0$  and  $\gamma = 4$  are measured for nearby galaxies, and  $\sigma_* = 225 \text{ km s}^{-1}$  is measured by fitting the observed separation distribution of lenses. This parameterization represents the “standard” model of Kochanek (1996) and Falco et al. (1998). Recent revisions to the model suggested by Chiba & Yoshii (1999) and Cheng & Krauss (1999) are generally inconsistent with the observations (see Kochanek et al. 1999). The probability that a source lies within the multiple-imaging region of a lens, also known as the optical depth, has a characteristic scale of  $\tau_* = 16\pi^3(\sigma_*/c)^4n_*r_H^3 = 0.026$  given the parameters for the mass and number of lens galaxies. Although the Hubble radius  $r_H = c/H_0$  enters the expression for the optical depth, the quantity  $r_H^3n_*$  is independent of the value of the Hubble constant. In a flat cosmological model, the optical depth is simply  $\tau = (\tau_*/30)(D_{OS}/r_H)^3$ , where  $D_{OS}$  is the comoving distance to the source (Turner 1990; see Carroll, Press & Turner 1992, Kochanek 1993b for general expressions). The average optical depth is closely related to the square of the observed image separations, with  $\tau \sim \langle \Delta\theta \rangle^2 n_* D_{OS}^3$  for all cosmologies and lens models. The characteristic image separation is  $\Delta\theta_* = 8\pi(\sigma_*/c)^2 = 2''.92$ , and in a flat cosmological model the average image separation is simply  $\langle \Delta\theta \rangle = \Delta\theta_*/2$ .

We use the soft X-ray (0.3–3.5 KeV) luminosity functions derived by Boyle et al. (1994), particularly their models H (for  $\Omega_0 = 1$ ) and K (for  $\Omega_0 = 0$ ). For an X-ray luminosity function  $dN/dLdz$ , the total number of unlensed X-ray sources brighter than flux  $S$  per unit solid angle is

$$\frac{dN}{d\Omega}(> S) = \int_0^\infty dV_s \int_{L_{min}}^\infty dL \frac{dN}{dLdz}(L) \quad (3)$$

where  $dV_s$  is the volume element, and  $L_{min} = 4\pi D_{lum}^2 S(1+z)^{\alpha-1}$  is determined from the luminosity distance  $D_{lum}$  and the spectral index  $\alpha$  defined by  $F_\nu \propto \nu^{-\alpha}$ . Boyle et al. (1994) use  $H_0 = 50 \text{ km s}^{-1} \text{ Mpc}^{-1}$ , and assume a fixed spectral index of  $\alpha = 1$ . In a flat cosmology the volume element is  $dV_s = D_{OS}^2 dD_{OS}$  where  $D_{OS}$  is the comoving distance to the source, and the luminosity distance is  $D_{lum} = D_{OS}(1+z_s)$  in all cosmologies. To find the number of lensed X-ray sources we must include the redshift-dependent optical depth and the magnification bias (see Schneider, Ehlers & Falco 1992), so the number of lensed X-ray sources in a flat cosmology is

$$\left( \frac{dN}{d\Omega} \right)_L (> S) = \int_0^\infty dV_s \tau(z_s) \int_{L_{min}}^\infty dL \int_{M_{min}}^\infty \frac{dM}{M} \frac{dP}{dM} \frac{dN}{dLdz} \left( \frac{L}{M} \right) C \left( \frac{\Delta\theta_{min}}{\Delta\theta_*} \right). \quad (4)$$

The number of lensed sources is related to the number of unlensed sources through the optical depth at a given source redshift  $\tau(z_s)$ , the magnification of the lensed sources relative to the unlensed sources as described by the magnification probability distribution  $dP/dM$ , and selection limits on the detectable image flux ratios and separations. For the SIS lens the probability distribution for the magnification is  $dP/dM = 8/M^3$  and the minimum detectable flux ratio  $f < 1$

sets the lower limit of the magnification integral,  $M_{min} = 2(1+f)/(1-f)$ . We must also eliminate the lenses with separations below the resolution limit of Chandra. The angular selection function

$$C(x = \Delta\theta_{min}/\Delta\theta_*) = 30 \int_0^1 du u^2 (1-u)^2 \exp(-x^2/u^2) \quad (5)$$

gives the fraction of lenses with separations larger than a minimum value  $\Delta\theta_{min}$ . The expressions for the optical depth and the volume element change for cosmological models with non-zero curvature (see Carroll et al. 1992 and Kochanek 1993b for general expressions). We present the results for the two cosmologies,  $\Omega_0 = 0$  and  $\Omega_0 = 1$ , for which the X-ray LF was derived by Boyle et al. (1994). The results for the  $\Omega_0 = 0$  model should be similar to those for a flat model with  $\Omega_0 = 0.5$  and a cosmological constant (see Carroll et al. 1992).

Figure 1 shows the expected number of X-ray sources and lensed X-ray sources per square degree as a function of flux assuming a perfect detector ( $f > 0$  or  $M_{min} = 2$ , and  $C(x) = 1$ ). Figure 2 shows the redshift distribution of the lensed and unlensed sources for integrations of 1, 10 and 100 ksec assuming an exposure time of  $(S/2.5 \times 10^{-13} \text{ ergs s}^{-1} \text{ cm}^{-2})^{-1}$  ksec for a  $5-\sigma$  point source detection (e.g., Jerius et al. 1997). The lensing probability peaks near  $S = 10^{-13} \text{ ergs s}^{-1} \text{ cm}^{-2}$ , which provides the best balance between magnification bias and source redshift. The magnification bias is highest for the brightest sources (steep number counts, far from the break in number counts), while the lens cross section is highest for faint sources (highest average redshift). For brighter sources the probability drops because of the low average source redshift and for fainter sources it drops because of the flattening of the number counts distribution. The peak lensing probability of 0.2–0.4% (depending on the cosmological model) is lower than for bright quasars (about 1%) but higher than for radio sources (about 0.1–0.2%). The total number of X-ray lenses is enormous, reaching roughly one per square degree for  $S > 10^{-15} \text{ ergs s}^{-1} \text{ cm}^{-2}$ . Particularly for the  $\Omega_0 = 1$  model, the predictions are underestimates because the luminosity function models underpredict the observed number counts of sources (see Boyle et al. 1994).

Observational selection effects determine the fraction of these lenses that can be found, so we next estimate the number of observable lenses per HRC or ACIS exposure. The fundamental problem with the Chandra Observatory for conducting a lens survey is the strong variation in the resolution with the distance from the field center. We estimate (from Kenter et al. 1997) that the radius encircling 50% of the energy is approximately  $r_{50} = 0''.5 + 6''.0(D/10')^2$  at a distance  $D$  from the field center. The minimum separation for recognizing multiple images can be approximated by a small multiple of  $r_{50}$ ,  $\Delta\theta_{min} = \xi r_{50}$  with  $1 < \xi < 2$ . Thus, we can define an effective area for the detection of multiply imaged X-ray sources by

$$\Delta\Omega_{eff}(\xi) = 2\pi \int_0^\infty D dD C(\xi r_{50}/\Delta\theta_*) \quad (6)$$

where  $C(x)$  is the angular selection function introduced in eqn. (5). We can use an upper limit to the integral of  $\infty$  rather than the physical detector size because the exponential cutoff in  $C(x)$  makes it unimportant. For reasonable count rates the best estimate is  $\Delta\Omega_{eff}(\xi = 1) = 0.012$

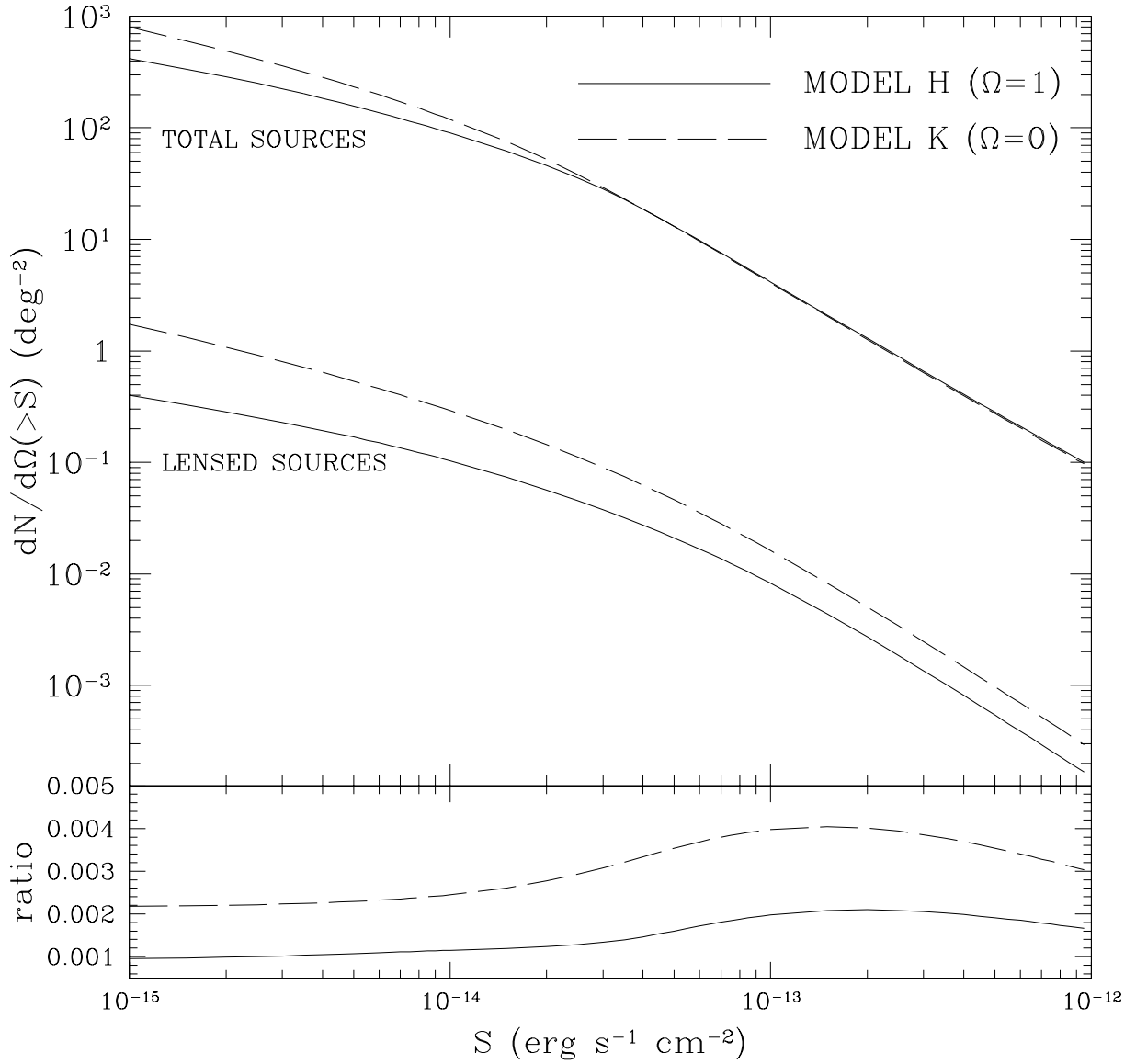


Fig. 1.— The number of unlensed (upper curves) and lensed (lower curves) X-ray sources brighter than flux  $S$  per square degree for either  $\Omega_0 = 1$  and LF model H (solid curves) or  $\Omega_0 = 0$  and LF model K (dashed curves) from Boyle et al. (1994). The lower panel shows the ratios of the curves, which are the fraction of all sources brighter than flux  $S$  that are gravitational lenses.

MODEL H ( $\Omega=1$ )

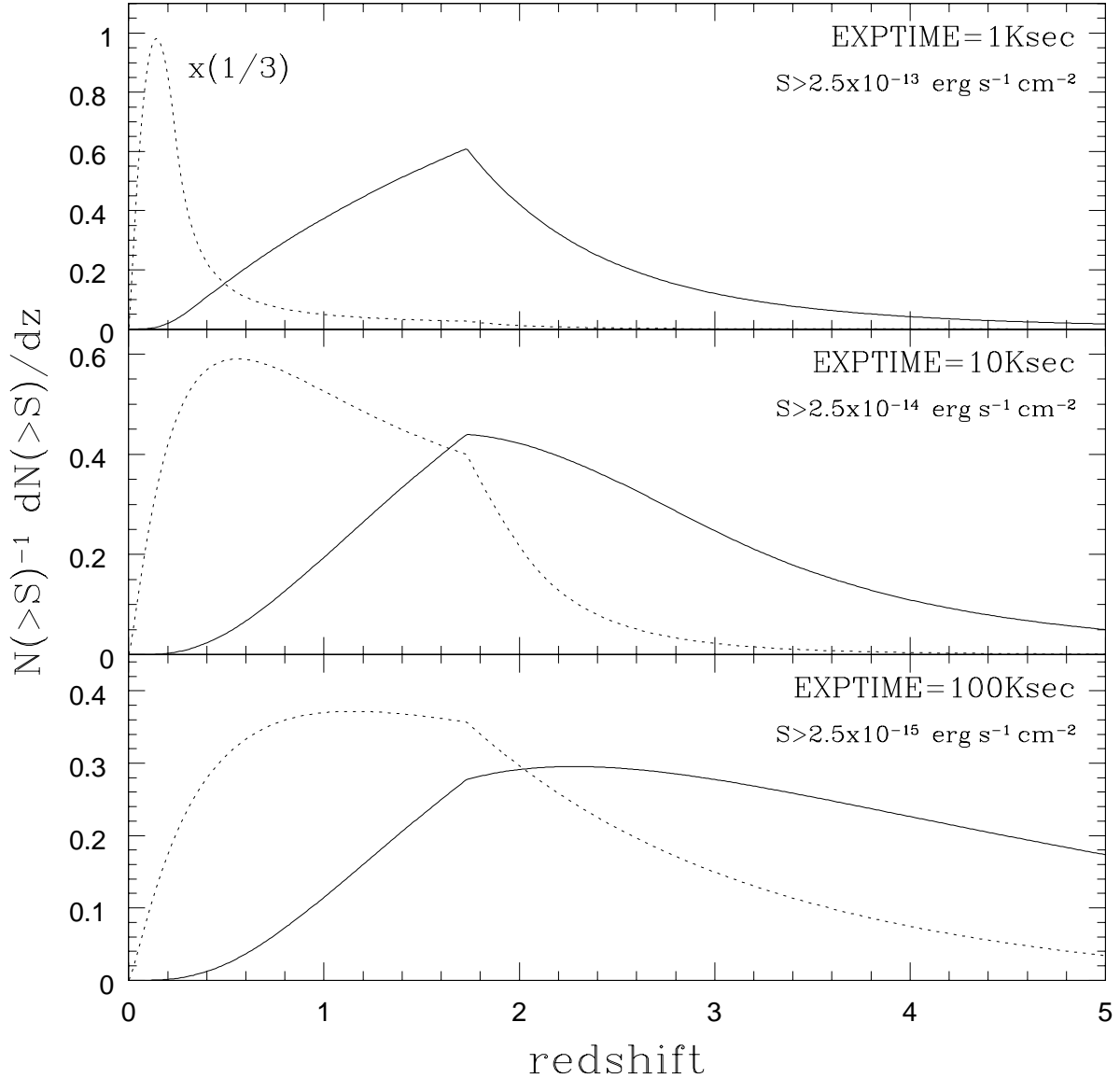


Fig. 2.— The normalized redshift distributions of unlensed (dashed) and lensed (solid) X-ray sources for typical exposure levels of 1, 10, and 100 ksec for  $\Omega_0 = 1$ . These distributions are independent of the selection function in flux ratio or separation.

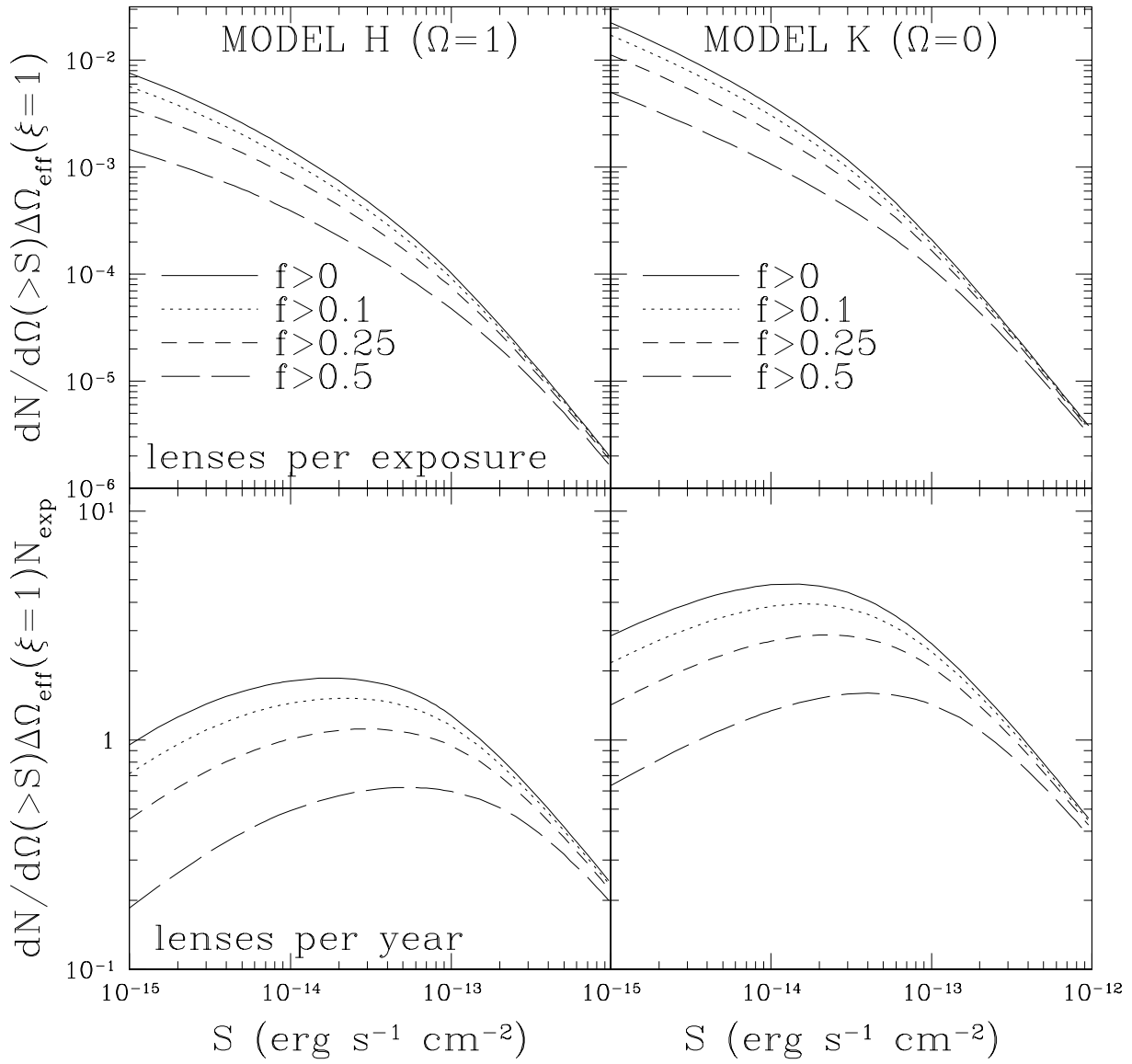


Fig. 3.— (Top) The number of lensed X-ray sources per telescope pointing including the effective area and flux ratio limits for  $\Omega_0 = 1$  and LF model H (left) and for  $\Omega_0 = 0$  and LF model K (right). (Bottom) The expected number of lenses per year of high resolution imaging including selection effects.

square degrees, but if pessimistic,  $\Delta\Omega_{eff}(\xi = 2) = 0.0035$  square degrees. Unfortunately, the effective area of the detector is far smaller than its total area. Figure 3 shows the expected number of lenses per telescope pointing (i.e. in an area  $\Delta\Omega_{eff}(\xi = 1)$ ) for limits on the detectable flux ratio of  $f > 0, 0.1, 0.25$  and  $0.5$ . The effect of the flux ratio limit is smallest for bright sources, where the magnification bias leads to a sample dominated by lenses with modest flux ratios, and enormous for faint sources. While the expected number of lenses drops rapidly as we move to brighter sources, the reduced exposure time needed to detect bright sources greatly increases the number of possible exposures. The number of exposures that can be taken per year is roughly  $N_{exp} = 10^4(S/10^{-13}\text{ergs s}^{-1}\text{cm}^{-2})$ , so the number of detectable lenses per year of high resolution imaging ( $\Delta\Omega_{eff}N_{exp}dN/d\Omega(> S)$ ) is roughly independent of the flux limit (see Figure 3). If the Chandra Observatory were devoted only to high resolution imaging, then we would expect to find 1–3 lenses per year.

### 3. CLUSTER LENSES

It is very unlikely to find a cluster acting as a lens in a randomly selected field (see Kochanek 1995, Wambsganss et al. 1995, Flores & Primack 1996, Maoz et al. 1997) – the high cross sections of clusters compared to galaxies are far outweighed by their rarity. However, many Chandra observations will be centered on intermediate redshift clusters, so they are pre-selected to have a massive, lensing object in the field. The critical radius scale for an SIS lens with velocity dispersion  $\sigma_c$  is  $b_* = 4\pi(\sigma_c/c)^2$ . For a particular lens and source redshift the image separation is  $\Delta\theta = 2b_*D_{LS}/D_{OS}$  for distances from the lens (observer) to the source of  $D_{LS}$  ( $D_{OS}$ ). The multiple-imaging cross section is  $\tau_c(z_s) = \pi\Delta\theta^2/4$ , so the expected number of lenses behind a cluster of velocity dispersion  $\sigma_c$  and redshift  $z_l$  is

$$N_c(> S) = \int_{z_l}^{\infty} dV_s \tau_c(z_s) \int_{L_{min}}^{\infty} dL \int_{M_{min}}^{\infty} \frac{dM}{M} \frac{dP}{dM} \frac{dN}{dL dz} \left( \frac{L}{M} \right), \quad (7)$$

where as before,  $dV_s = D_{OS}^2 dD_{OS}$  for a flat cosmology. The expected number of lenses  $N_c$  is very weakly dependent on the cosmological model (because the cross section depends only on the distance ratio  $D_{LS}/D_{OS}$ ), so we restricted the calculation to  $\Omega_0 = 1$  and luminosity function  $H$ . Even so, the number of lenses is underestimated because the LF model underestimates the number of faint X-ray sources. The image separations produced by a massive cluster are sufficiently large to allow us to assume that no systems are lost due to limitations in angular resolution, although we must still impose limits on the detectable flux ratios. Figure 4 shows the number of lenses expected behind a typical “giant-arc” cluster (velocity dispersion  $\sigma_c = 1200 \text{ km s}^{-1}$ ) at redshift  $z_c = 0.4$  as a function of the image flux ratio limit  $f$ . The expected number of lensed sources is roughly equal to the number of X-ray sources expected within solid angle  $\pi b_*^2$  – while the average cross section is smaller than  $\pi b_*^2$ , the magnification bias compensates. Figure 5 shows the expected number of lenses found in 1, 10 and 100 ksec images of clusters as a function of their redshift and velocity dispersion. As in the serendipitous surveys, individual observations are unlikely to detect

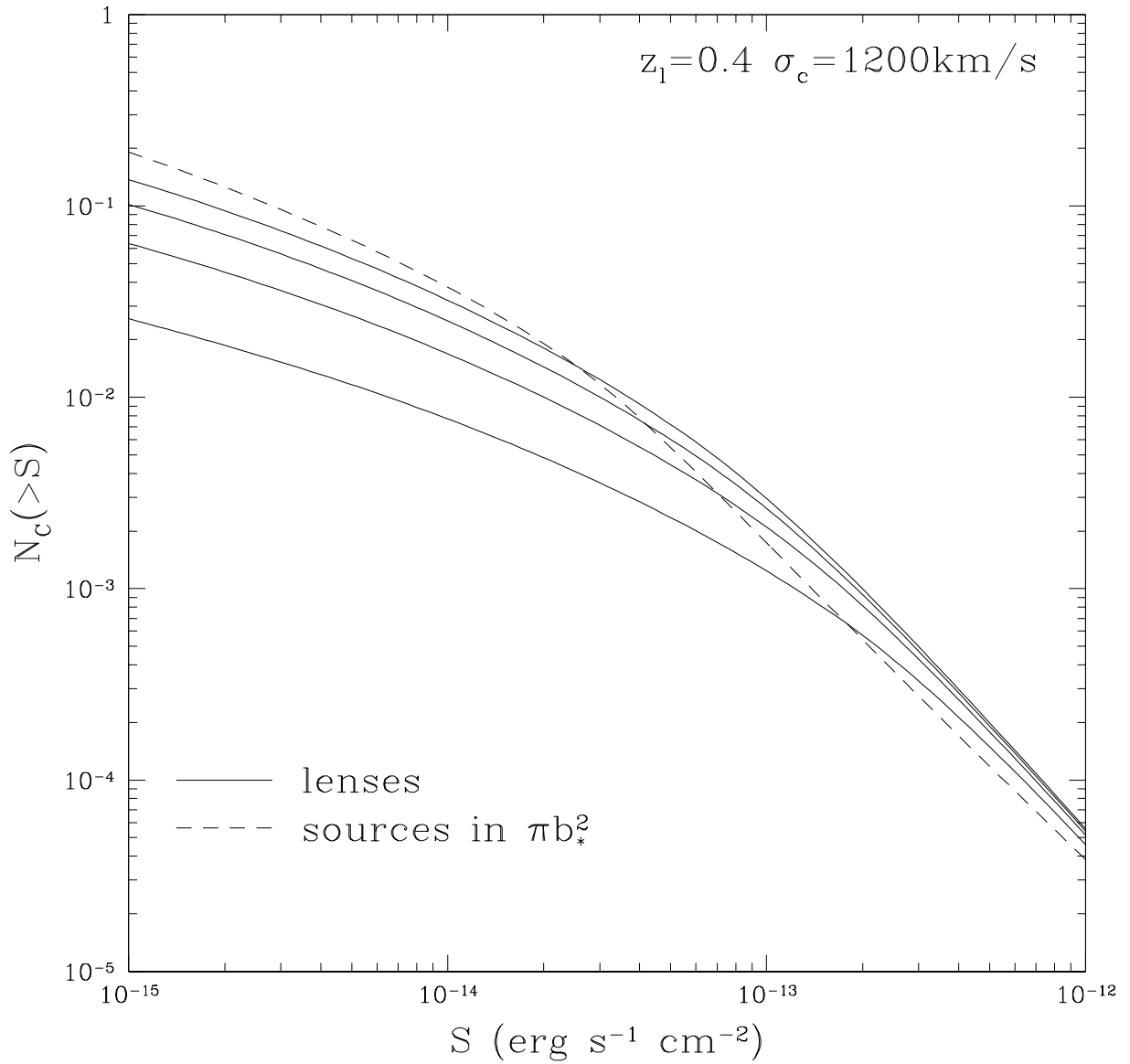


Fig. 4.— The number of multiply-imaged X-ray sources as a function of flux behind a typical cluster containing giant arcs, with  $z_l = 0.4$  and  $\sigma_c = 1200 \text{ km s}^{-1}$ . The solid lines show the expected number of lensed images brighter than flux  $S$  with limits on the detectable flux ratio of  $f > 0, 0.1, 0.25$  and  $0.5$  (top to bottom). The dashed line shows the number of sources which would be found within solid angle  $\pi b_*^2$  in the absence of any lensing effects.

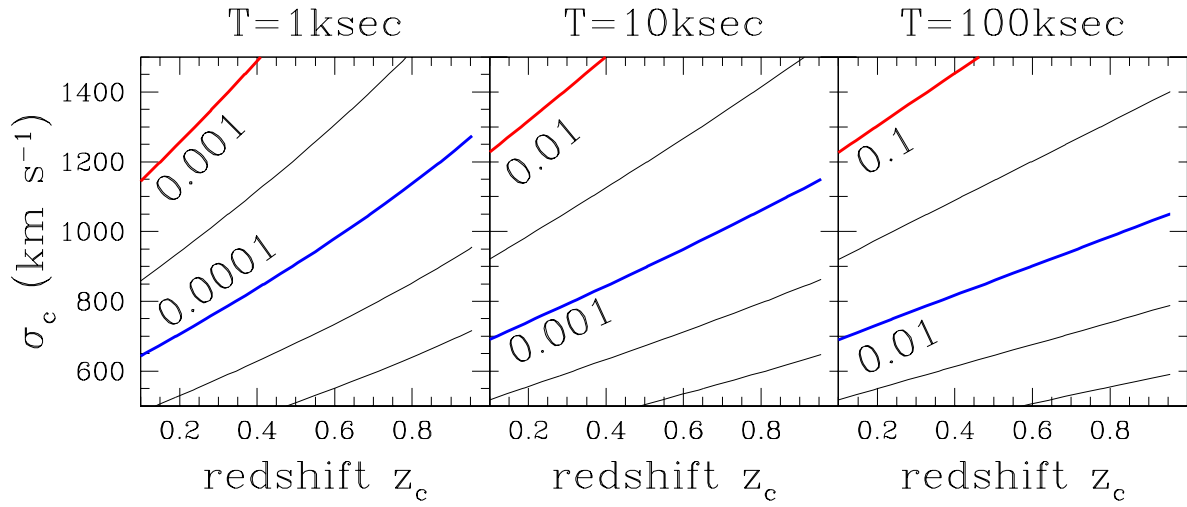


Fig. 5.— Contours of the expected number of lenses with flux ratios  $f > 0.5$  as a function of cluster redshift and velocity dispersion for exposure times of 1 ksec (left), 10 ksec (middle), and 100 ksec (right). Contours are spaced at intervals of 0.5 dex (a factor of  $\sim 3$ ), with labels on the heavy, shaded contours. The increase in the number of detections for weaker flux ratio restrictions can be determined from Figure 4.

multiply-imaged systems, but the accumulated results of all imaging programs will find lensed sources. The number of lenses detected is of order 1–10 for each year devoted to imaging clusters, depending on the mass and redshift distributions of the clusters. Whether the SIS is a realistic representation of cluster lenses is an open question (e.g. see Williams, Navarro & Bartelmann 1999), but the cross section estimates should be approximately correct.

#### 4. SUMMARY

The Chandra X-ray Observatory will discover both serendipitous lenses, where a random background source is found to be lensed by a foreground galaxy, and cluster lenses, where a background source is found to be lensed by a cluster that is the target of a Chandra pointed observation. The number of detectable systems is 1–3 serendipitous lenses and 1–10 cluster lenses per year of imaging time, roughly independent of the flux limit of the observations and including strong limits on the detectability of the lensed images. These are probably *underestimates* because the Boyle et al. (1994) luminosity functions we used for our calculations undercount the numbers of X-ray sources at faint flux limits. The X-ray Multi-Mirror Mission (XMM, <http://astro.estec.esa.nl/XMM>), with its coarser angular resolution (5''.0 FWHM), will be unable to detect gravitational lenses produced by galaxies. However, its high sensitivity will make it very useful for detecting cluster lenses.

The total number of lensed X-ray sources is enormous, roughly  $(10^{-15} \text{ ergs s}^{-1} \text{ cm}^{-2} / S)$  lenses per square degree brighter than a soft X-ray flux  $S$ , with none of the confusion problems which interfere with searches for gravitational lenses in the optical or radio. An X-ray telescope with the resolution of the Chandra Observatory over a wide field of view would be an extraordinarily efficient instrument for finding gravitational lenses. Alternatively, deep, high resolution optical images of X-ray sources should be an efficient means of searching for new gravitational lenses.

Acknowledgments: We would like to thank Adam Dobrzycki for comments and for producing simulated HRC images of gravitational lenses. We would also like to thank Richard Mushotzky and Xavier Barcons for their comments. CSK is supported by NASA ATP grant NAG5-4062.

#### REFERENCES

Barkana, R., Lehár, J., Falco, E. E., Grogin, N. A., Keeton, C. R. & Shapiro, I. I. 1999, ApJ, in press (astro-ph/9808096)

Bernstein, G. & Fischer, P. 1999, ApJ, in press (astro-ph/9903274)

Boyle, B. J., Shanks, T., Georgantopoulos, I., Stewart, G. C. & Griffiths, R. E., 1994, MNRAS, 271, 639

Carroll, S. M., Press, W. H. & Turner, E. L. 1992, *ARA&A*, 30, 499

Cheng, Y.-C. N. & Krauss, L. M. 1999, *astro-ph/9810393*

Chiba, M. & Yoshii, Y. 1999, *ApJ*, 510, 42

Cooray, A.R., 1999, *A&A*, 342, 353

Fabbiano, G. 1989, *ARA&A*, 27, 87

Faber, S. & Jackson, R. E. 1976, *ApJ*, 204, 668

Falco, E.E., Kochanek, C.S. & Muñoz, J.A., 1998, *ApJ*, 494, 47

Fassnacht, C. D. et al. 1999, *AJ*, 117, 658

Flores, R.A. & Primack, J.R., 1996, *ApJ*, 457, 5L

Griffith, M., Heflin, M., Conner, S., Burke, B. & Langston, G. 1991, *ApJS*, 75, 801

Helbig, P. 1999, *astro-ph/9904311*

Helbig, P., Marlow, D., Quast, R., Wilkinson, P. N., Browne, I. W. A. & Koopmans, L. V. E. 1999, *A&AS*, 136, 297

Impey, C. D., Falco, E. E., Kochanek, C. S., Lehár, J., McLeod, B. A., Rix, H.-W., Peng, C. Y. & Keeton, C. R. 1998, *ApJ*, 509, 551

Jerius, D., Zhao, P., Van Speybroek, L., Tennant, A., Swartz, D., Schwartz, D. A., Podgorski, W. A., Harris, B., Graessle, D. E., Gaetz, T. J., Freeman, M. D., Elsner, R., Edgar, R. J. & Cohen, L. M. 1997, *BAAS*, 190.2901

Keeton, C. R., Kochanek, C. S., & Falco, E. 1998, *ApJ*, 509, 561

Kenter, A.T., Chappell, J.H., Kobayashi, K., et al., 1997, *Proc. SPIE*, 3114, 26

King, L. J. & Browne, I. W. A. 1996, *MNRAS*, 282, 67

Kochanek, C. S., Falco, E. E., Impey, C. D., Lehár, J. L., McLeod, B. A., & Rix, H.-W. 1999, “After the Dark Ages: When Galaxies Were Young”, 9th Maryland Astrophysics Conference, editors S. Holt and E. Smith, AIP conference proceedings 470, page 163, (AIP: New York)

Kochanek, C. S. 1996, *ApJ*, 473, 595

Kochanek, C.S., 1995, *ApJ*, 453, 545

Kochanek, C. S. 1993a, *ApJ*, 417, 438

Kochanek, C. S. 1993b, *MNRAS*, 261, 453

Luppino, G. A., Gioia, I. M., Hammer, F., Le Fèvre, O. & Annis, J. A. 1999, *A&AS*, 136, 117

Maoz, D., Rix, H.-W., Gal-Yam, A., & Gould, A., 1997, *ApJ*, 486, 75

Rix, H.-W., de Zeeuw, P.T., Cretton, N., van der Marel, R.P., & Carollo, C.M. 1997, *ApJ*, 488, 702

Schechter, P. 1976, *ApJ*, 203, 297

Schneider, P., Ehlers, J. & Falco, E. E. 1992, in “Gravitational Lenses”, Springer-Verlag, Berlin

Turner, E.L., 1990, *ApJ*, 365, L43

Wambsganss, J., Cen, R., Ostriker, J.P. & Turner, E.L., 1995, *Science*, 268, 274

Williams, L.R.L, Navarro, J.F. & Bartelmann, M., 1999, *astro-ph/9905134*